JOURNAL OF AGRICULTURAL AND FOOD CHEMISTRY

Comparative Lipidomics of Four Strains of *Saccharomyces cerevisiae* Reveals Different Responses to Furfural, Phenol, and Acetic Acid

JIN-MEI XIA AND YING-JIN YUAN*

Key Laboratory of Systems Bioengineering, Ministry of Education, School of Chemical Engineering and Technology, Tianjin University, P.O. Box 6888, Tianjin 300072, People's Republic of China

To reveal differences between inhibitor-resistant *Saccharomyces cerevisiae* strains and their parental strain and to investigate the response of *S. cerevisiae* to furfural, phenol, and acetic acid, comparative lipidomics strategy was employed using an LC-ESI/MS^n technique on four *S. cerevisiae* strains, which include an industrial strain (SC) and three tolerant strains screened by this laboratory by step adaptation—a furfural-tolerant strain (SCF), a phenol-tolerant strain (SCP), and an acetic acid-tolerant strain (SCA). Lipidome data were then analyzed using wavelet transform-principal component analysis (WT-PCA). Results revealed that phosphatidylcholines (PCs), phosphatidylinositols (PIs), and phosphatidic acids (PAs) were biomarkers for discriminating SC from SCF, SCP, and SCA, respectively. PIs were believed to be extraordinarily important in all inhibitor-tolerant processes because they were the biomarkers responsible for the discrimination of all four different strains. Further analysis of the distribution of different hydrocarbon chains revealed that both the saturation and the length of the chains helped in maintaining proper fluidity of membranes.

KEYWORDS: Yeast; inhibitor; lipidome; WT-PCA; ESI-MS

INTRODUCTION

Using plant biomass to produce ethanol is the most promising strategy to overcome the resource crisis (*1*). During the process of converting the cellulose and hemicellulose fractions of plant biomass to fermentable sugars (*2*), various compounds such as furans, aromatics, and low molecular weight organic acids are inevitably generated (*3*). These compounds are potent inhibitors for microorganisms such as *Saccharomyces cerevisiae* used in the following fermentation procedures. Among these inhibitors, furfural, phenol, and acetic acid (*4, 5*) gained the most attention. They were found to inhibit the growth and ethanol production rate of yeast. Because both removal of the inhibitors and detoxification of pretreated hydrolysates (*6*) led to higher production cost (*7*), in the industrial context, developing robust and inhibitor-tolerant production organisms became a prerequisite.

Scientists have made efforts to obtain inhibitor-tolerant strains from *S. cerevisiae* (*8*). Martin et al. (*9*) have proved that under both low and high concentrations of inhibitors the adapted strain could get higher ethanol yield and higher specific ethanol productivity, and the adapted strain also showed stronger ability in converting inhibitors into less toxic compounds. Keating et al. (*10*) revealed that the tolerant strains were faster in consuming sugars and furfural and also in producing ethanol. However, all of these studies were focused on downstream parameters such as the ethanol yield, ethanol productivity, glucose consumption rates, and so on (*11*); the immediate responses of cells were rarely considered.

Russell et al. (*12*) pointed out that membrane lipids were the most adaptable molecules in response to environmental changes and were the targets in stress adaptation. The composition changes of both the acyl chains and the polar head groups can alter the packing arrangements of the lipids and can thus affect the bilayer stability and fluidity, sometimes even the lipid−protein interactions. Lei et al.'s work (*13*) related the composition of plasma membrane to the ethanol tolerance of *S. cerevisiae*. Mannazzu et al.'s research (*14*) also revealed that the lipid composition and membrane integrity played important roles during *S. cerevisiae*'s adaptation to unfavorable environmental conditions. Under such circumstances, investigating the changes of membrane lipids under the stress of furfural, phenol, and acetic acid became rather intriguing. The variety of the polar groups and the length or number of unsaturated double bonds in the associated fatty acids made the lipids that comprise the bilayer matrix of the cell membranes very complex (*15*), and this complexity of phospholipids (PLs) demands the profiling of the entire spectrum of lipids or lipidome of *S. cerevisiae*. Thanks to the development of high-throughput equipment, especially the technological advances in lipid analysis, the yeast lipidomics approach (*16*), targeting the characterization on a quantitative level of all lipids in cells or tissues, can now be easily realized. In this paper, the lipidomes of three tolerant strains of *S. cerevisiae* domesticated by our laboratory together with an industrial *S. cerevisiae* strain were profiled using

* Corresponding author (fax 86-22-27403888; e-mail yjyuan@tju.edu.cn or yjyuan@public.tpt.tj.cn).

10.1021/jf802720t CCC: $40.75
Published on Web 12/02/2008

comparative lipidomics strategy. Their responses to furfural, phenol, and acetic acid on the lipidome level were investigated.

MATERIALS AND METHODS

Materials. 1,2-Dimyristoyl-*sn*-glycero-3-phospho-*rac*-(1-glycerol) (sodium salt) (14:0/14:0 PG), 1,2-dilauroyl-*sn*-glycero-3-phosphoethanolamine (12:0/12:0 PE), 1,2-dilauroyl-*sn*-glycero-3-phosphocholine (12:0/12:0 PC), L-α-phosphatidylinositol (PI) sodium salt from bovine liver, 1,2-dimyristoyl-*sn*-glycero-3-phospho-L-serine sodium salt (14:0/14:0 PS), and 1,2-dimyristoyl-*sn*-glycero-3-phosphate (sodium salt) (14:0/14:0 PA) were purchased from Avanti Polar Lipids (Alabaster, AL). Chloroform and methanol were of HPLC grade from Merck (Darmstadt, Germany). Ammonium hydroxide (28−30%) was from J and K Chemical.

Yeast extract peptone dextrose (YPD) medium was made of 10 g/L yeast extract, 20 g/L peptone, and 20 g/L glucose, whereas the YPD solid medium had another 20 g/L of agar. High-sugar YPD medium had quite a similar composition except that the content of glucose was 100 g/L. Extraction liquid was a chloroform/methanol mixture, 2:1 by volume, with 0.01% butylated hydroxytoluene (BHT) as the antioxidant. The liquid for dissolving the sample was also a chloroform/methanol mixture, 1:1 by volume, with 0.01% BHT. Internal standards mixture was made of PG, PE, PC, PI, PS, and PA as mentioned above with each component at a concentration of 0.1 mg/mL. Mobile phase A was made of chloroform, methanol, and ammonium hydroxide, 89.5:10:0.5 by volume, and mobile phase B was made of chloroform, methanol, water, and ammonium hydroxide, with a ratio of 55:39:5.5:0.5.

Strains and Inhibitors. A strain of *S. cerevisiae*, baker's yeast (SC) from Angel Yeast Corp., was used in the experiment. To get a furfural-tolerant strain, SC was cultivated in YPD medium with furfural. The concentration of furfural was controlled to be high enough to kill a big proportion of the cells. After cultivating for 24 h, the cells were transferred to a solid YPD medium without furfural. The surviving colonies were then transferred to liquid YPD medium containing furfural and were cultivated for at least five generations in this medium to ensure the tolerant capacity was stable. The adaptation process was performed successively using YPD medium with increasing furfural contents until no cell could survive the high furfural concentration. Strains with different furfural-tolerant capacities were obtained. The furfural-tolerant strain (SCF) used in this experiment could survive 15 mL/L (0.18 mol/L) furfural. A phenol-tolerant strain (SCP) and an acetic acid-tolerant strain (SCA) were also obtained using this adaptation and screening procedure. The SCP strain could survive a phenol concentration as high as 8 g/L (0.085 mol/L), whereas the SCA strain could survive an acetic acid concentration of 35 mL/L (0.6 mol/L). The strains were maintained on YPD solid medium stored at −4 °C and were transferred to fresh plates every 2 months.

Usually the inhibitor concentrations used to test their effects on fermentation were 10−100 times (*17*) that of the concentration found in the hydrolysates. As described by Martinez et al. (*18*), the concentration of acetic acid can be as high as 5.3 ± 2.99 g/L (about 0.088 ± 0.05 mol/L) in the hemicellulose hydrolysates. This was followed by phenolic compounds with a concentration of 2.86 ± 0.34 g/L (about 0.03 ± 0.0036 mol/L). The concentration of furans, which equaled 1.305 ± 0.288 g/L (0.0135 ± 0.003 mol/L), was the lowest of the three. The amount of furfural was then chosen as a standard. Because the furfural-tolerant strain can survive a furfural concentration of 0.18 mol/L, the final furfural concentration used was set at 0.15 mol/L. The concentrations of acetic acid and phenol were decided accordingly to ensure that the three have similar inhibitory effects on cell growth. The amounts of acetic acid and phenol were then set at 0.3 and 0.04 mol/L, respectively.

Inoculum. Inocula for lipid extraction were grown in a three-stage process. First, a loopful of SC cells was transferred from an agar slant to a 250 mL eight-layer-gauze plugged conical flask, which contained 50 mL of YPD medium; incubation was carried out in an orbital incubator (Jeiotech, Kyonggido, Korea) at 160 rpm and 30 °C for 12 h. Then, a portion of this culture was transferred to 450 mL of medium in a 2 L eight-layer-gauze plugged conical flask to achieve a starting cell density with an optical density (measured at 600 nm, OD_{600}) equal to 0.3 and a final volume of around 500 mL. This culture was then incubated in an orbital incubator (DHZ-C, Jiangsu, China) at 90 rpm and 30 °C for 8 h. After that, a portion of this culture was transferred to 400 mL of high-sugar-YPD medium in a 2 L eight-layer-gauze plugged conical flask to achieve an OD_{600} of 0.35 and a final volume of around 450 mL. Two duplicates were prepared in this step. When this culture was grown for about 6 h and reached an OD_{600} equal to 4, which corresponds to midexponential phase for the strains used, 6.2 mL of furfural was sterilized by filtration and dissolved in 50 mL of medium and added to one flask to make the furfural concentration in the flask approximately 0.15 mol/L. As references, blank medium with the same composition, but without any inhibitors, was added to another flask. To investigate the immediate and short-term responses of the cells to inhibitors on the lipidome level, and also to ensure the concentrations of inhibitors were still high when sampling, samples for lipidome analysis were withdrawn at 0, 20, and 60 min after the addition of the medium. SCF culture flasks were prepared according to the same procedure. Comparative studies were also carried out for SC versus SCP and SC versus SCA in the same procedures except that the final inhibitor concentrations were 0.04 mol/L of phenol and 0.3 mol/L of acetic acid, respectively.

Extraction of Phospholipids from Cell Membrane. The extraction procedure was optimized after comparison of the efficiency of Folch's (*19*), Bligh and Dyer's (*20*), and Wenk's (*21*) methods. Furthermore, to improve the recovery of those PLs with higher polarity, acetic acid solution (0.05%) (*22*) was used during the extraction process. The cells were separated from the medium through filtration immediately after sampling and were then washed by deionized water three times. After that, the cells were transferred into a fresh glass tube containing 1.5 mL of extraction liquid, 0.6 mL of acetic acid solution (0.05%), and 10 μL of internal standards solution. The mixture was then vibrated twice using a vortex agitator for 30 s to make the cells contact well with the extraction liquid. Another 3 mL of extraction liquid was added to the mixture, and the tube was vibrated for 30 s two more times. The tube was then centrifuged for 5 min at a speed of 94*g* to get a three-layer system with the cells in the middle. The bottom layer was then removed using a pipet. This extraction procedure (the addition of 3 mL of extraction liquid followed by vibration and centrifugation and removal of the bottom layer) was repeated three to five times until the cells sank to the bottom after centrifugation. After the last centrifugation (when the cells were at the bottom of the tube), the liquid phase was also collected. After that, 0.5 mL of 1 M KCl was added to the collected liquid and vibrated for 30 s to wash the extract. This was followed by centrifugation for 3 min at a speed of 376*g*, and the upper phase was discarded after centrifugation. Then 1 mL of water was used to further wash the extract. The remaining liquid was then dried under nitrogen. The residue was redissolved with the 1:1 chloroform methanol mixture containing 0.01% BHT and stored at −20 °C until analysis.

LC Separation. PL separations were obtained on a 150 mm × 4.6 mm i.d. column packed with Hypersil Si (5 μm particle size, Phenomenex, Torrance, CA) with a guard column made of the same packing material at 25 °C. The mobile phase consisted of eluents A and B. The linear gradient realized by a Waters (Milford, MA) 600 pump was as follows: from 0 to 7 min, eluent B was changed from 5 to 20%; 20% eluent B was kept for 3 min; from 10 to 15 min, eluent B was changed from 20 to 30%; from 15 to 45 min, eluent B was changed from 30 to 50%; from 45 to 50 min, eluent B was changed from 50 to 5%; and eluent B was kept at 5% for 5 min. The total chromatographic run cycle time was 55 min. The volume of the extracted samples injected into the LC-ESI-MS/MS system was 10 μL, and injections were carried out with a Waters 717 autosampler. The flow rate was 1 mL/min, and the eluent from the column was split to ensure that a 0.2 mL/min flow was directed into the ion source of the mass spectrometer.

Mass Spectrometry Analyses. Mass spectrometry analysis of the samples was performed using a Waters Quattro Micro API mass spectrometer. Further MS^2 and MS^3 analyses were realized using a Finnigan LCQ Advantage ion-trap mass spectrometer (Thermo Electron, San Jose, CA) under conditions as reported in our previous work (*23*). For MS analysis, the ESI parameters for negative ion detection were optimized before LC injections by infusing a PLs standards mixture

using a syringe pump with pure mobile phase A at 0.2 mL/min. The capillary voltage was set at 3.0 kV, the source temperature was set at 120 °C, and the desolvation temperature was set at 350 °C. The scan speed was 1000 *m*/*z* units per second, and the scan was carried out over a range of *m*/*z* 500−1000. Nitrogen was used as sheath and auxiliary gas. CID experiments were acquired using helium as collision gas.

Data Acquisition. When used in single-stage MS mode, relative peak intensities of different PLs classes mainly depend on the lipid concentrations of the samples analyzed. A single molecular ion with a mass-to-charge ratio (*m*/*z*) characteristic for the molecular weight was present for each molecular. Collision-induced dissociation of the peaks of interest yields fragmentation patterns, which were used to unambiguously identify the lipid(s) present at a particular *m*/*z* value.

Mass chromatograms were used to calculate the peak areas for each PL molecule. The amount of each PL molecule was calculated according to the peak area of the lipid standard in each group. All peaks were integrated using Quanlynx (version 4.1) software from Waters.

The relative quantifications of PLs were performed using a mixture of 14:0/14:0 PG, 12:0/12:0 PE, 12:0/12:0 PC, L-α-phosphatidylinositol (PI) sodium salt from bovine liver, 14:0/14:0 PS, and 14:0/14:0 PA as the internal standard (IS); the cell pellets were spiked with 10 μL of the stock solution (0.1 mg/mL for each component) of the standards mixture before the extraction step.

Ratios of sample peak areas to internal standard peak areas (ordinate) were plotted against ratios of nominal analyte concentrations to internal standard concentrations (abscissa), and calibration curves were calculated by least-squares linear regression without weighting. The resulting slope of the calibration curve was then used to calculate the concentration of the respective analyte in the samples according to the equation

$$C_{\text{analyte}} = \frac{S_{\text{analyte}}}{S_{\text{internal}}} \times C_{\text{internal}} \div \text{slope} \qquad (1.1)$$

where $S_{\text{analyte}}$is the peak area of the analyte, S_{internal} is the peak area of the internal standard, C_{internal} is the concentration of internal standard, and C_{analyte} is the concentration of analyte.

Multivariate Statistical Analysis. Data matrices with each column representing a specific PL molecule and each row representing a sample with the value being concentrations (nmol of PLs/mg of sample) were analyzed. To minimize the influence of different levels for different lipid groups, each value for a certain species of PLs was divided by the total amount of the specific group of PLs it was in. The data matrix was then denoised using wavelet transform (WT) as described in our previous work (*24*) before principal component analysis (PCA). The score plots and loading plots generated from WT-PCA were then used to judge the differences and similarities between samples and the corresponding biomarkers responsible for discrimination.

RESULTS

Effect of Furfural, Phenol, and Acetic Acid on *S. cerevisiae* Cell Growth. Under control conditions (specified as "C" in **Figure 1**), the growth of four *S. cerevisiae* strains showed differences, with SC having the greatest potential and arriving at the highest stationary phase cell density of about 10.7 (cell density was evaluated by optical density at 600 nm (OD_{600}) in this paper if not specified otherwise). This was followed by SCF, which was able to get a quite similar stationary phase cell density of about 10.3. The final cell densities for SCA and SCP were a little lower, with their OD_{600} values being about 9.6 and 9.3, respectively.

Both SC and SCF were inhibited in growth after the addition of furfural (specified as "F" in **Figure 1**). The growth of SC was more severely inhibited, with a stationary phase cell density being reduced to an OD_{600} of about 7.3, whereas for SCF that value was about 8.6. When compared with their control conditions, the decreases of stationary cell density for SC and SCF were 3.4 (~31.8%) and 1.7 (~16.5%), respectively. This

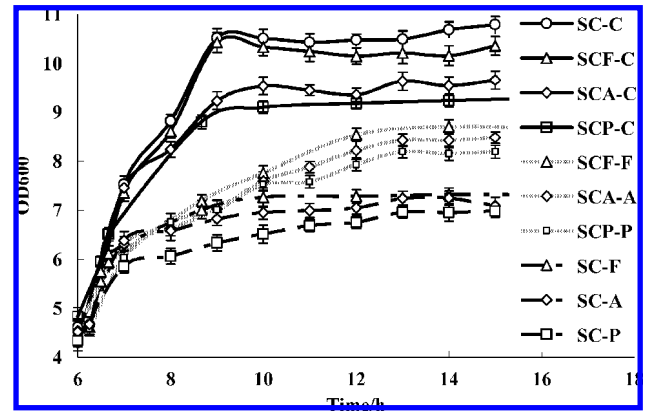

Figure 1. Growth curve for four *Saccharomyces cerevisiae* strains. SC, SCF, SCA, and SCP represent the names of the four strains, whereas C, F, A, and P represent the "control condition", "after the addition of furfural", "after the addition of acetic acid", and "after the addition of phenol", respectively. All inhibitors were added to the culture at 6 h after cultivation (the first time point for each curve in the figure). Error bars represent standard deviations; where not seen, they lie within the symbol ($n \geq 3$).

offered strong evidence for SCF's stronger resistance to furfural. The addition of acetic acid (specified as "A" in **Figure 1**) also inhibited the growth of both SC and SCA, with SC being inhibited more severely. When compared with their control condition, the decreases of stationary cell density for SC and SCA were 3.5 (~32.7%) and 1.2 (~12.5%), respectively. Similarly, the addition of phenol (specified as "P" in **Figure 1**) led to lower final cell densities for both SC and SCP. The decreases of final cell density for them induced by phenol were 3.7 (~34.6%) and 1.1 (~11.8%), respectively. All three resistant strains showed lower growing activity than SC under control conditions, whereas after the addition of inhibitors, they all showed higher growth rates and higher final cell densities, indicating that they were more tolerant to inhibitors than SC.

Profiling of Phospholipids for Four Strains of *S. cerevisiae*. Under the LC conditions described above, six groups of PLs were separated following a sequence of PG (phosphatidylglycerol), PE (phosphatidylethanolamine), PC (phosphatidylcholine), PI (phosphatidylinositol), PS (phosphatidylserine), and PA (phosphatidic acid). Mass spectrometry analysis together with MS^2 and MS^3 analyses totally uncovered the structures of 120 species of PLs, which include 9 species of PGs, 24 species of PEs, 25 species of PCs, 30 species of PIs, 17 species of PSs, and 15 species of PAs (for further information see the Supporting Information). The 92 species were further quantified according to eq 1.1. General analysis of the species information revealed that different groups of lipids had different levels of carbon chain diversities. Analysis of the distributions of the hydrocarbon chains showed that palmitic acid(C16:0) and stearic acid (C18:0) were the most predominant carbon chains in *S. cerevisiae*, whereas palmitoleic acid (C16:1) and oleic acid (C18:1) were the major unsaturated species. This was in accordance with the study carried out by Wagner and Platauf (*25*).

Further quantitative analysis (**Table 1**) of PLs for the four *S. cerevisiae* strains revealed that PCs were the predominant PLs in *S. cerevisiae*, accounting for >48% in each strain. This was followed by PE and PI, with each accounting for about 20%. The levels for the three minor species, PS, PA, and PG, were all <10%. This was in accordance with Daum's work (*26*).

When compared with SC, SCF showed higher levels of PCs together with lower levels of PEs and PIs, whereas for SCP,

Table 1. Comparison of Phospholipid Composition (Mean ± SD[a]) for Four *S. cerevisiae* Strains

		phospholipid group					
strain		PG	PE	PC	PI	PS	PA
SC	amount/(nmol/mg)	0.82 ± 0.03	8.46 ± 0.19	18.26 ± 0.5	6.44 ± 0.22	2.21 ± 0.06	1.28 ± 0.03
	relative abundance/%	2.18 ± 0.07	22.6 ± 0.5	48.73 ± 1.34	17.18 ± 0.59	5.89 ± 0.17	3.42 ± 0.08
SCF	amount/(nmol/mg)	0.94 ± 0.04	8.68 ± 0.36	21.71 ± 0.88	7 ± 0.28	2.33 ± 0.09	1.47 ± 0.06
	relative abundance/%	2.23 ± 0.11	20.61 ± 0.86	51.53 ± 2.08	16.61 ± 0.66	5.52 ± 0.22	3.5 ± 0.15
SCP	amount/(nmol/mg)	0.77 ± 0.02	7.13 ± 0.35	17.44 ± 0.7	6.93 ± 0.34	2.07 ± 0.06	1.07 ± 0.05
	relative abundance/%	2.16 ± 0.06	20.15 ± 0.98	49.27 ± 1.96	19.56 ± 0.97	5.85 ± 0.18	3.01 ± 0.14
SCA	amount/(nmol/mg)	0.95 ± 0.04	10.21 ± 0.5	21.54 ± 0.73	7.15 ± 0.33	2.64 ± 0.09	1.77 ± 0.07
	relative abundance/%	2.14 ± 0.09	23.06 ± 1.14	48.67 ± 1.64	16.16 ± 0.76	5.96 ± 0.2	4 ± 0.16

[a] SD, standard deviation ($n \geq 3$).

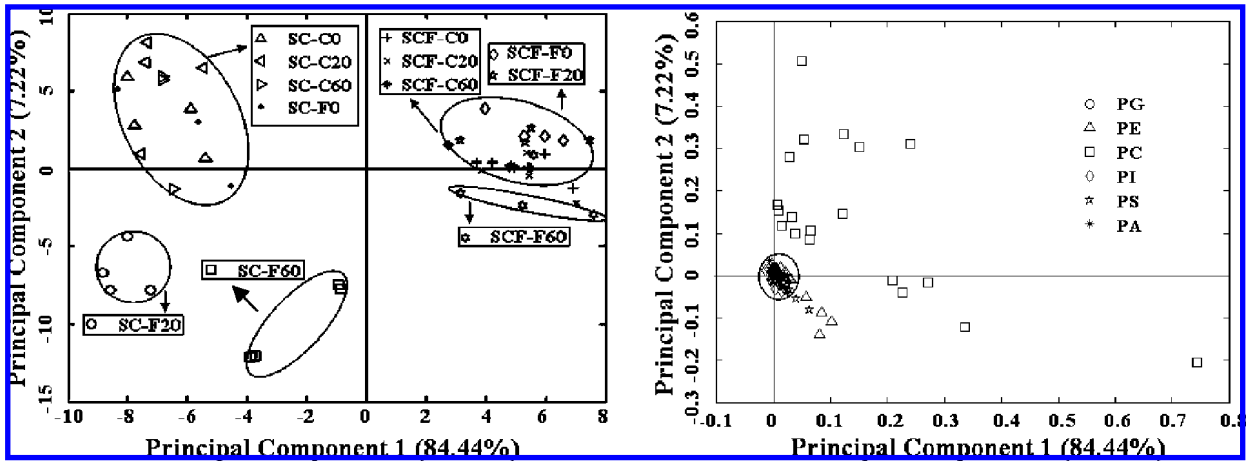

Figure 2. Multivariate statistical analysis of lipidome data for SC and SCF using WT-PCA: (**A**) score plot for SC and SCF on the first two principal components; (**B**) loading plot for SC and SCF on the first two principal components. C0, C20, and C60 represent the control samples, which were sampled at 0, 20, and 60 min after the addition of blank medium. F0, F20, and F60 represent samples that were sampled at 0, 20, and 60 min after the addition of furfural.

together with the lower levels of PEs and PAs, were the higher levels of PCs and PIs. The different changing trends for PIs in SCF and SCP suggested that they might have different mechanisms for inhibitor tolerance. In SCA, the relative abundance for PIs decreased while at the same time the levels for PEs and PAs increased, with PAs changing in the most significant way.

Multivariate Statistical Analysis Using WT-PCA. *Discrimination of SC and SCF Samples.* The score plot from the lipidome data of SC and SCF in **Figure 2A** showed the similarities and differences of samples. The control samples for SC and SCF under all three time points gathered together, respectively, indicating that the changes of lipidome along time for both strains were not that significant after the addition of blank medium. Interestingly, for SC, at both 20 and 60 min, samples taken after the addition of furfural can be discriminated from the control samples, whereas for SCF, almost all of the samples distributed in a small area; only samples taken at 60 min after the addition of furfural were a little farther from other SCF samples. This indicated that the impact of furfural for SC begins no later than 20 min after its addition, whereas for SCF only subtle changes can be detected after 60 min of furfural addition. Furthermore, the discrimination of SC and SCF under control conditions was mainly realized by the first principal component (which contributed 84.44% to the total variances); that is, SC and SCF samples were discriminated from each other on the abscissa as is shown in **Figure 2A**, whereas the discrimination of SC samples before and after the addition of furfural was mainly realized by the second principal component (ordinate, which contributed 7.22% to the total variances). Because the first principal component (abscissa) contributed much more to the total variances than the second principal component (ordinate), it can be concluded that the difference made by the addition of furfural (mainly reflected from the ordinate) was not as significant as the difference existing between the two strains (mainly exemplified from the abscissa).

The corresponding loading plot (**Figure 2B**) showed that the possible biomarkers for distinguishing various samples were phosphatidylcholines (PCs), which have been implicated in a number of specific cell biological processes and play important roles in signal transduction (*27*). PCs are the most abundant glycerophospholipids in yeast and can spontaneously organize into bilayers (*28*) thanks to their overall cylindrical molecular shape, which makes them very important in protecting cells. In our research, when compared with SC, the relative contents of unsaturated PC species for SCF were lower (**Figure 3A**). Higher amounts of PC28:0, PC30:0, PC32:1, PC32:0, and PC34:1 together with lower amounts of PC28:1, PC30:2, PC32:2, and PC34:2 were observed in SCF. For each group of PCs with the same hydrocarbon chain length, an increase of saturation for hydrocarbon chains was observed. In each group, a higher amount of saturated fatty acids was accompanied by a lower amount of monounsaturated fatty acids, whereas a higher amount of monounsaturated fatty acids was always accompanied by a lower amount of polyunsaturated fatty acids. The changes of PLs represented an adaptive membrane alteration compensating for the direct physicochemical interaction of furfural with the

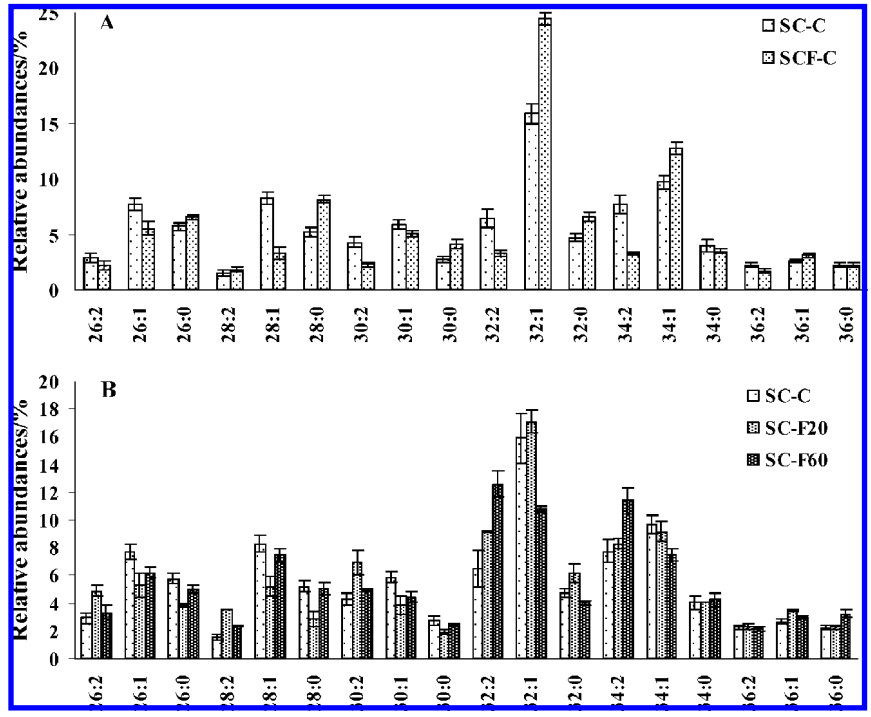

Figure 3. Relative abundances for different PC molecules: (**A**) relative abundances for different species of PCs in SC and SCF; (**B**) changes of PC molecules for SC after the addition of furfural. Error bars represent standard deviations; where not seen, they lie within the symbol ($n \geq 3$).

cell membrane. This adaptive response of membrane lipids was probably the biochemical basis for tolerance to furfural.

As for SC (**Figure 3B**), at 20 min after the addition of furfural, increases of PC26:2, PC28:2, and PC30:2 together with decreases of PC26:0, PC28:1, PC28:0, and PC30:1 were observed, whereas at 60 min, increases of PC32:2 and PC34:2 together with decreases of PC32:1, PC32:0, and PC34:1 were observed. The addition of furfural increased the unsaturation for short-chain PLs at 20 min with the long-chain ones hardly changed. At 60 min the levels for short-chain PLs resumed, whereas the unsaturation levels for long-chain PLs increased. It can be concluded that the influence of furfural after 20 min of its addition was mainly on the short-chain PLs, whereas its long-term effect was on the long-chain PLs. Ramos et al.'s work (*29*) also revealed that the toxic compounds had both short- and long-term effects on *Pseudomonas putida*. At both time points, there was an increase of unsaturated PLs. The relative content for different PC molecules in SCF (data not shown) did not change that much at 20 min after furfural addition. At 60 min after the addition of furfural, the relative abundance of those polyunsaturated PC species was higher than the control condition but not that much. This strongly suggested that the influence of furfural to SCF's membrane was not that significant.

Discrimination of SC and SCP Samples. The score plot (**Figure 5A**) generated from the lipidome data of SC and SCP after WT-PCA exhibited five groups of samples. Samples for SC were divided into three groups, with those sampled after the addition of phenol at 20 and 60 min forming two separate groups and other samples forming one group. For SCP, samples at 60 min after the addition of phenol were discriminated from other SCP samples. This also offered strong evidence that the resistant capabilities to phenol for SC and SCP were quite different, with the latter being much stronger. Furthermore, the discrimination of SC and SCP under control conditions was mainly realized on the first principal component (contributing 61.19% to the total variances), whereas samples before and after the addition of phenol were discriminated on the second principal component (contributing 21.60% to the total variances). This was similar to the case of furfural's influences on SC and SCF. The differences between SC and SCP under control conditions were not the same as the differences made by the addition of phenol.

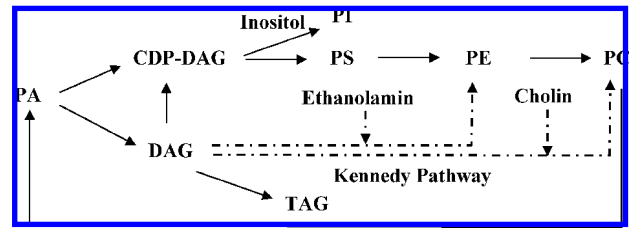

Figure 4. Schematic representation of metabolic network for phospholipids. DAG, 1,2-diacylglycerol; CDP, cytidine diphosphate; TAG, triacylglycerides.

The biomarkers which distinguished the samples of SC from those of SCP were mainly PIs, which can be generated from PA via the CDP-DAG pathway (**Figure 4**; see **Figure 5B** for prevalence of PIs). For both minor species (**Figure 6B**) and major species (**Figure 6A**) of PIs, a decrease of short hydrocarbon chain molecules and an increase of long hydrocarbon chain molecules were observed in SCP when compared with SC under control conditions. PIs, which are abundant in membrane and possess the biggest diversity among the six groups, are important molecules both in maintaining membrane structure and in generating signal transduction molecules. They can be rapidly synthesized and degraded in discrete membrane domains or even subnuclear structures and thus are ideal regulators of very dynamic cell processes. The major species of PIs usually distributed on the cytoplasmic side of the plasma membrane bilayer. Although how PIs work to convey the phenol tolerance was still unclear, it was clear that PIs played an important role in leading to the differences between SC and SCP in resisting phenol.

Discrimination of SC and SCA Samples. From the score plot generated from lipidome data for SC and SCA (**Figure 7A**) we

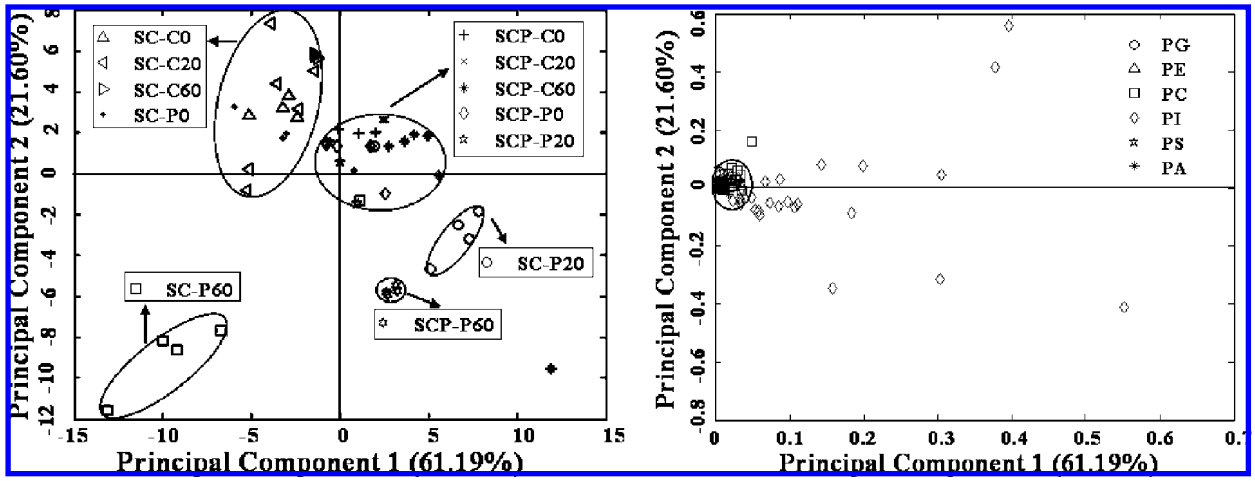

Figure 5. Multivariate statistical analysis of lipidome data for SC and SCP using WT-PCA: (**A**) score plot for SC and SCP on the first two principal components; (**B**) loading plot for SC and SCP on the first two principal components. C0, C20, and C60 represent the control samples, which were sampled at 0, 20, and 60 min after the addition of blank medium. P0, P20, and P60 represent samples that were sampled at 0, 20, and 60 min after the addition of phenol.

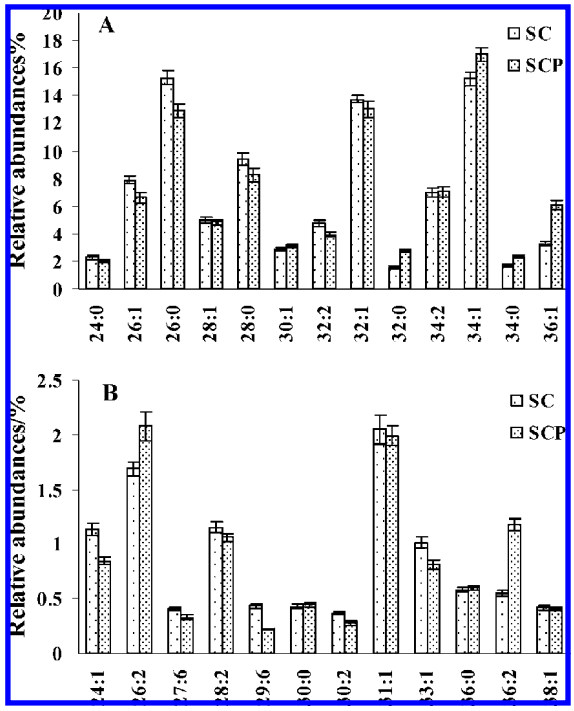

Figure 6. Relative abundances for different PI molecules: (**A**) relative abundances for major species of PIs in SC and SCP; (**B**) relative abundances for minor species of PIs in SC and SCP. Error bars represent standard deviations; where not seen, they lie within the symbol ($n \geq 3$).

can see that samples of SC at 20 and 60 min after the addition of acetic acid were discriminated from other SC samples, whereas for SCA only samples at 60 min after the addition of acetic acid were discriminated from other SCA samples. This revealed that for SC the treatment with acetic acid made a difference from 20 min, whereas for SCA, this difference was not shown until 60 min. As a contrast to the difference made by treatment of acetic acid, the two strains showed no significant difference under control condition. This was quite different from the cases for SCF and SCP.

The loading plot (**Figure 7B**) showed that PAs were the possible biomarkers for discriminating SC and SCA samples. PAs are the central precursor for the synthesis of four groups of glycerolphospholipids, including PEs, PCs, PIs, and PSs (indicated with solid lines in **Figure 4**). This made this relatively small group of PLs very important in regulating the behaviors of the cells. The relative content of different PA molecules changed after treatment with acetic acid for both SC and SCA. For SC, the most significant change happens on PA32:2, PA34:2, and PC34:1, with the former decreased with time while the latter two increased. This indicated that under acetic acid stress SCs tended to form more long-chain lipids to protect themselves, whereas for SCA, the biggest changes happened in PA32:2, PA32:0, PA34:2, and PA34:0, with decreasing PA32:2 and PA34:2 and increasing PA32:0 and PA34:0; that is, the C16:0 and C18:0 increased while the C16:1 and C18:1 decreased. This offered a clue that for SC the influence of acetic acid was on the length of the hydrocarbon chains of PAs, whereas for SCA the influence was on the saturation of the chains of PAs. The different changing trends for PAs offered important clues for different responding mechanisms for SC and SCA. Because the amount of PAs in *S. cerevisiae* cell membranes was rather low, it was believed that the changes of PAs were more of a kind of signal event than a kind of structural change for the membrane.

Discrimination of All Samples. When the lipidome data of SC, SCF, SCP, and SCA were put together, multivariate statistical analysis using WT-PCA also got interesting results. From the score plot of all the samples (**Figure 9A**), samples of SC at 60 min after the addition of furfural, phenol, and acetic acid each formed separate groups. Samples of SCP sampled at 60 min after the addition of phenol fell into a different group. Samples of SCF under control conditions and those sampled after the addition of furfural at all time points together with SC samples at 0 and 20 min after the addition of furfural formed another group. Similarly, both SC and SCP samples sampled at 0 and 20 min after the addition of phenol together with samples of SCP under control conditions gathered in one group. The control SCA samples, SCA samples sampled at all time points after the addition of acetic acid together with control SC samples, and SC samples at 0 and 20 min after the addition of acetic acid formed another group. This indicated that the additions of furfural, phenol, and acetic acid all led to significant changes of SC after treatment for 60 min, thus making their discrimination from the control samples and samples sampled

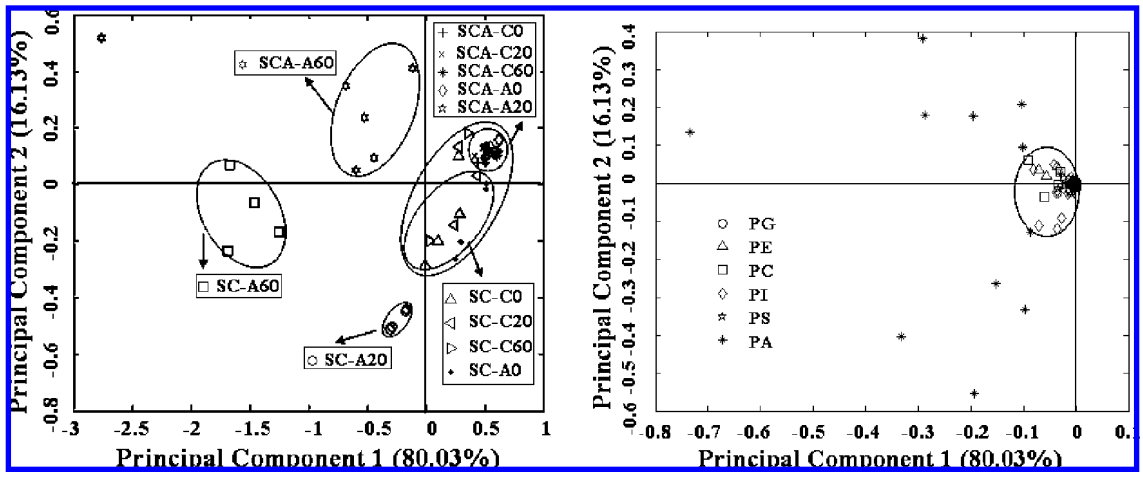

Figure 7. Multivariate statistical analysis of lipidome data for SC and SCA using WT-PCA: (**A**) score plot for SC and SCA on the first two principal components; (**B**) loading plot for SC and SCA on the first two principal components. C0, C20, and C60 represent the control samples, which were sampled at 0, 20, and 60 min after the addition of blank medium. A0, A20, and A60 represent samples that were sampled at 0, 20, and 60 min after the addition of acetic acid.

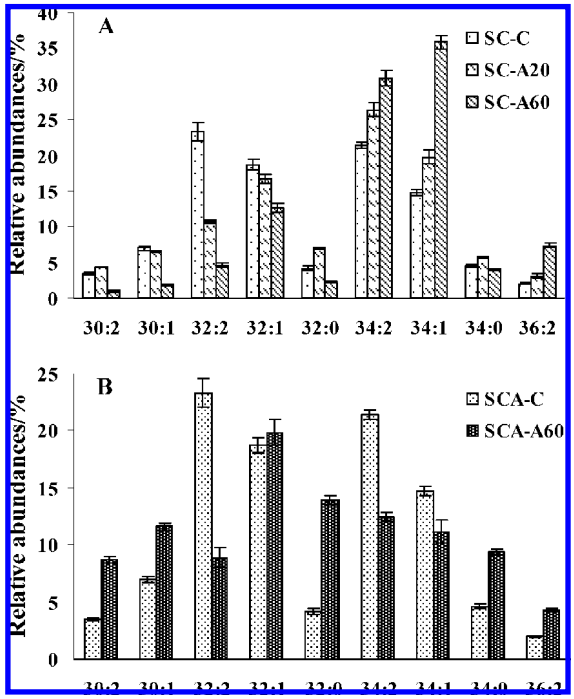

Figure 8. Distribution of PAs in yeast: (**A**) distribution of PAs in SC after treatment with acetic acid; (**B**) distribution of PAs in SCA after treatment with acetic acid. Error bars represent standard deviations; where not seen, they lie within the symbol ($n \geq 3$).

at 20 min. The score plot also showed that control samples of SC were more similar to SCA than to the other two resistant strains.

Further loading plot analysis (**Figure 9B**) indicated that PIs together with some species of PEs, PAs, and PCs were possible biomarkers. The biomarkers for the discrimination of all the samples were more complex than cases for discrimination between two strains. Probably this happened because different resistant strains respond differently to corresponding inhibitors, but PIs were the predominant biomarkers. Through phosphorylation in several positions by different kinases PIs can further be metabolized into phosphatidylinositol 4-monophosphate [PI(4)P] and phosphatidylinositol 4,5-bisphosphate [PI(4,5)P2], which are important signal molecules in cells (*30*). PI(4)P can interact with some cytoskeletal proteins such as talin, whereas PI(4,5)P2 is a very important substrate for different phosphalipase C (PLC). PIs can further generate DAG and, after phosphorylation by DAG-kinases, can then generate PAs, which might have a role as second messengers. The importance of PIs also relies on the fact that the synthesis of PC is coordinately regulated with the synthesis of PI, mediated by genetic and biochemical mechanisms (*31*). In fact, when the synthesis of PCs was inhibited thanks to the loss of free cholines, PIs together with PEs were believed to make up for the loss of PCs (*32*). It was reported (*33*) that in *S. cerevisiae*, inositol and choline regulate the genes encoding PL-synthesizing enzymes. Except for the process of membrane biogenesis, inositol and choline are also involved in various metabolic pathways such as biotin synthesis, cell wall organization and biogenesis, and acetyl-CoA metabolism. All of these roles for PIs made them very important in all three inhibitor-tolerant processes.

DISCUSSION

Applying metabolomics to solving agricultural problems has already been posed by Dixon et al. (*34*). The agriculture-produced cellulosic materials were widely believed to be the best potential raw materials for producing ethanol, and inhibitors such as furfural, phenol, and acetic acid generated from the hydrolysis process of these raw materials became the biggest obstacles for further fermentation processes. The resistant strains developed by our laboratory showed higher viability than the parental strain, which is now widely used in ethanol-producing factories in China. In this paper, lipidomics, a branch of metabolomics strategy, was carried out in a relatively well-defined culture system. One hundred and twenty species of PLs were identified in this research. Although it has been a long time since *S. cerevisiae* became the target of PL research, our research is the first attempt to offer PL profiling information for *S. cerevisiae* membrane.

The most attractive and powerful aspect of "omics" approaches was their ability of profiling all or as much as possible molecules or substances simultaneously. To generate information from these overwhelming data, the multivariate statistical analysis technique together with the high-throughput equipment became the two legs of the systematic approach. In our research, the PL data were analyzed using the data-mining method WT-PCA. WT was introduced to denoise the data, and PCA further offered the gathering of sample information via score plots and biomarker information via the loading plots.

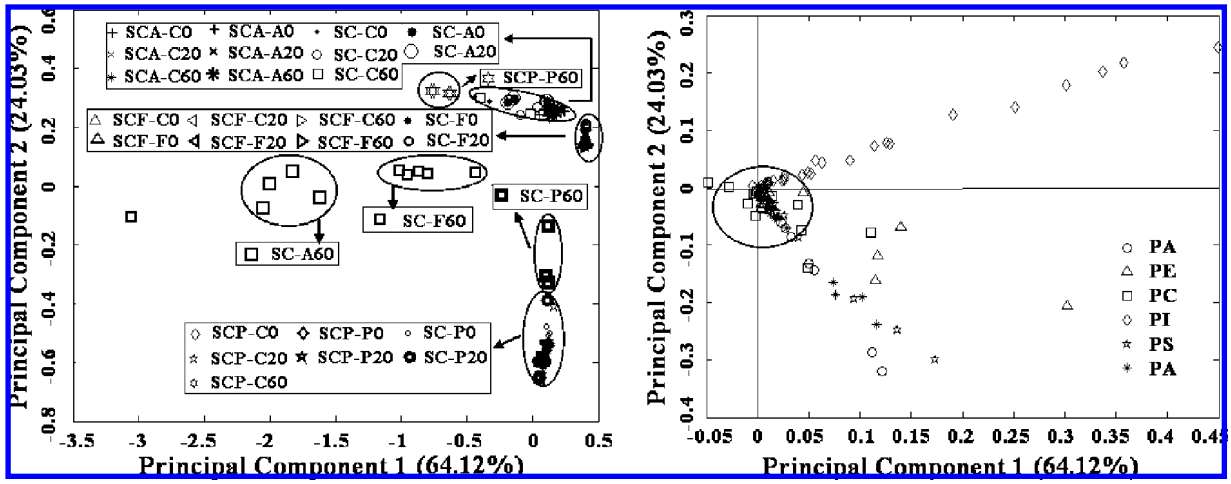

Figure 9. Multivariate statistical analysis of lipidome data for all of the samples using WT-PCA: (**A**) score plot of all samples on the first two principal components; (**B**) loading plot of all samples on the first two principal components. F60, P60, and A60 represent samples that were sampled at 60 min after the addition of furfural, phenol, and acetic acid, respectively.

In our research, the addition of inhibitors changed the composition of cell membrane phospholipids. Strains with different capacities in resisting inhibitors showed differences in membrane phospholipids profiling. For each set of data, the score plot divided the samples into intelligible groups; that is, on the lipidome level samples from tolerant strains can be discriminated from SC samples. These facts strongly support our belief that the changes of lipids play an important role in conveying the tolerance. This notion was also backed up by various papers in the literature such as Mannazzu's work (*14*) and Turk's work (*35*).

The loading plots from WT-PCA offered us information about responsible biomarkers. The biomarkers for the discrimination of SC with SCF, SC with SCP, and SC with SCA were PCs, PIs, and PAs, respectively. These biomarkers were believed to play important roles in conveying inhibitor tolerance.

PCs can be synthesized in *S. cerevisiae* cells with the enzyme PE-*N*-methyl-transferase from PEs after three sequential methylation steps (*36*). They can also be synthesized from free cholines through the CDP-choline (Kennedy) pathway (indicated with dashed lines in **Figure 4**), which is located at the cytosolic side of the endoplasmatic reticulum (*37*). It was previously reported that in *S. cerevisiae* the methylation of PEs and the CDP-choline route contributed differently to the steady-state profile of PC species (*27*). Whereas the methylation of PEs produced predominantly the diunsaturated PC species PC32:2 and PC34:2 and the CDP-choline-derived PCs are enriched in the monounsaturated species PC32:1 and PC34:1, the relatively higher amounts of PC32:1, PC34:1, and PC36:1 together with the lower amounts of PC32:2, PC34:2, and PC36:2 offered us a clue that SCF mainly got its PCs from the CDP-choline pathway. As shown in **Figure 4**, although the consumption of PEs for producing PCs through methylation was decreased, the higher consumption of DAG through the Kennedy pathway for PC synthesis became a competition for synthesis of PEs via the Kennedy pathway. This was backed up by the higher levels of PCs together with lower levels of PEs (**Table 1**). Furthermore, the resources of PCs supported the hypothesis that additional cholines were helpful for cells in the process of furfural stress tolerance.

The different responses of SC and SCF were probably caused by the changes of acyl chain saturation. The increase of unsaturated PL level always led to an increase of the membrane fluidity (*35*). This can be taken as a clue for SCF's stronger resistance to furfural. Pepi et al.'s work (*38*) showed that the arsenic-resistant bacterial strains react to the stress of arsenic by changing the composition of their membrane fatty acids. They also proved that the decreasing growth rate was correlated with the increasing saturation of the membrane fatty acids. Our findings showed similar trends. SCF showed lower growth activity than SC and higher levels of saturated membrane fatty acids.

Interestingly, although the furfural-tolerant strain SCF was obtained from SC via adaptation to increasing levels of furfural, when compared with control samples of SC, the changing of PC profiles for control SCF samples and SC samples after the addition of furfural showed quite different trends. For SC samples after the addition of furfural, higher levels of unsaturated PCs were observed, whereas control SCF samples had higher levels of saturated PCs than SC control samples. As Ingram (*39*) proved that cell membrane responded to ethanol through incorporation of more unsaturated fatty acids into phospholipids, which would increase membrane fluidity, del Castillo Agudo (*40*) reported that ethanol tolerance was correlated to a decrease in the fatty acid unsaturation index. As has been proved (*41*), hydrophobic compounds were able to partition into the lipid bilayer, and this partition was influenced not only by the nature of the compound but also by the density of the membrane. It has also been verified that the accumulation of these compounds into membranes involved the change of membrane PLs, which allows the microorganisms to keep an optimal fluidity (*42*). Although SC cells responded to furfural through increasing PC unsaturation and membrane fluidity, which was a kind of adaptation, this may also make the insertion of furfural into the membrane bilayers easier, which led to a further increase of membrane fluidity. As cells that increased the unsaturation of their PCs failed to tolerate increasing levels of furfural, probably those having opposite trends managed to survive and finally became tolerant strains. Because their starting PC unsaturation level was low, they offered greater potential for the increase of unsaturation level if needed.

PIs are responsible for the discrimination of SC with SCP. Opposite trends for short hydrocarbon chain molecules (decreasing) and long hydrocarbon chain molecules (increasing) were observed in SCP. It was reported that the two most important factors influencing the fluidity of membranes were the saturation of the membrane lipids and the length of the hydrocarbon chains for lipids (*12*). The lengthening of the acyl chains of PLs led to

lower membrane fluidity. An increase of saturation for PCs was also observed for SCP when compared with SC (data not shown), although the change was not that significant. The higher levels of saturated PLs were similar to the case for SCF, and it can be concluded that higher levels of PL saturation for both SCF and SCP offered them greater potential for further increasing of unsaturation of membrane lipids.

Furthermore, when compared with SC strains, the levels of PAs and PEs were lower for SCP (**Table 1**). This was believed to be caused by an enhancement of their transformation into PIs and PCs as indicated in **Figure 4**. Studies on the genome level revealed that some glycerophospholipid synthesis genes were maximally expressed when inositol was absent from the growth medium and repressed when inositol was added to the growth medium (*33*). Because the formation of PIs needs the participation of inositols, higher levels of PIs will accompany a consumption of inositols in medium. This inositol consumption then gave rise to the synthesis of inositol (**Figure 6**). The new synthesized inositols not only compensated the consumed part but also formed a reservoir for extra needs. For strains of SCF and SCA, the total amount of glycerophospholipids is higher than that of the SC strain, whereas for the SCP strain, the total amount is a little lower (**Table 1**). This can be explained as extra inositols causing the repression of the synthesis of the glycerophospholipids and thus leading to a lower level of total amount of PLs in SCP.

PAs, biomarkers responsible for distinguishing SC and SCA, can be generated via the turnover of PC (**Figure 4**). They can also be synthesized from PI-generated DAG. Boumann's research revealed that the "Kennedy pathway" (indicated with dashed lines in **Figure 4**) and DAG pathway contributed differently to molecule species (*27*) and thus verified that neither of these two pathways can be substituted by the other. This fact together with the central role in the DAG pathway made PAs a group of very important metabolites in PL biosynthesis and membrane remodeling. Our previous work on *Taxus cuspidata* cells (*43*) also revealed that the formation of PAs was an important signaling response of cells to outer elicitors.

Interestingly, from the score plots, both the furfural-tolerant strain SCF and the phenol-tolerant strain SCP showed significant difference from their parental strain SC, whereas the acetic acid-tolerant strain SCA was quite similar to SC from the lipidome level. When all of the samples were put together, the score plot also showed that control samples of SC were more similar to SCA than to the other two resistant strains. Furthermore, for tolerant strains, only the addition of phenol led to apparent changes to SCP at 60 min. These differences were believed to be caused by the different toxicities of the different inhibitors. Many studies on various animal organelles such as liver microsomes and enzymes have found a linear increase in toxicity or inhibitory action to cells in a series of compounds as their log P_{ow} (octanol−water partition coefficient) increases. The log P_{ow} value for phenol is 1.46, that for furfural is 0.41, and that for acetic acid is −0.17. Phenol is much more lipophilic than furfural and acetic acid, and this can explain its relatively higher toxicity because phenol exhibited similar inhibitory effects to cells with the lowest amount (0.04 mol/L) when compared with furfural (0.15 mol/L) and acetic acid (0.3 mol/L). Because acetic acid is rather hydrophilic, which is different from furfural and phenol, this made the adaptation of membrane to it more subtle, involving changes of PLs in a relatively less significant way. Similarly, the hydrophobic property of phenol and its corresponding powerful influence toward membrane led to the discrimination of SCP samples at 60 min after phenol addition.

Although the biomarkers responsible for the discrimination of resistant strains with SC were different, the resistant strains did share some common features. PIs were believed to be extraordinarily important. Anyway, different phospholipid groups are not isolated, which can well explain the complexity of biomarkers when all samples were put together. In general, our study confirmed that the addition of different inhibitors influenced the fluidity of cell membranes, and proper membrane fluidity was of crucial importance for tolerance against inhibitor stress. It was believed that both the saturation and the length of hydrocarbon chains of phospholipids were important for regulating membrane fluidity.

ABBREVIATIONS USED

S. cerevisiae, *Saccharomyces cerevisiae*; SC, industrial strain of *S. cerevisiae*; SCF, furfural-tolerant strain of *S. cerevisiae*; SCP, phenol-tolerant strain of *S. cerevisiae*; SCA, acetic acid-tolerant strain of *S. cerevisiae*; YPD, yeast extract peptone dextrose; BHT, butylated hydroxytoluene; HPLC, high-performance liquid chromatogram; ESI, electrospray ionization; WT-PCA, wavelet transform-principal component analysis; PL, phospholipid; IS, internal standard; PG, phosphatidylglycerol; PE, phosphatidylethanolamine; PC, phosphatidylcholine; PI, phosphatidylinositol; PS, phosphatidylserine; PA, phosphatidic acid; DAG, 1,2-diacylglycerol; CDP, cytidine diphosphate; TAG, triacylglycerides.

Supporting Information Available: Phospholipids identified in *Saccharomyces cerevisiae* and score plot of all samples. This material is available free of charge via the Internet at http://pubs.acs.org.

LITERATURE CITED

(1) Chang, M. C. Y. Harnessing energy from plant biomass. *Curr. Opin. Chem. Biol.* **2007**, *11*, 677–684.
(2) Orts, W. J.; Holtman, K. M.; Seiber, J. N. Agricultural chemistry and bioenergy. *J. Agric. Food Chem.* **2008**, *56*, 3892–3899.
(3) Klinke, H. B.; Thomsen, A. B.; Ahring, B. K. Inhibition of ethanol-producing yeast and bacteria by degradation products produced during pre-treatment of biomass. *Appl. Microbiol. Biotechnol.* **2004**, *66* (1), 10–26.
(4) Szengyel, Z.; Zacchi, G. Effect of acetic acid and furfural on cellulase production of *Trichoderma reesei* RUT C30. *Appl. Biochem. Biotechnol.* **2000**, *89* (1), 31–42.
(5) Palmqvist, E.; Grage, H.; Meinander, N. Q.; Hahn-Hagerdal, B. Main and interaction effects of acetic acid, furfural, and *p*-hydroxybenzoic acid on growth and ethanol productivity of yeasts. *Biotechnol. Bioeng.* **1999**, *63* (1), 46–55.
(6) Persson, P.; Andersson, J.; Gorton, L.; Larsson, S.; Nilvebrant, N. O.; Jonsson, L. J. Effect of different forms of alkali treatment on specific fermentation inhibitors and on the fermentability of lignocellulose hydrolysates for production of fuel ethanol. *J. Agric. Food Chem.* **2002**, *50* (19), 5318–5325.
(7) Vonsivers, M.; Zacchi, G.; Olsson, L.; Hahnhagerdal, B. Cost-analysis of ethanol-production from willow using recombinant *Escherichia coli*. *Biotechnol. Prog.* **1994**, *10* (5), 555–560.
(8) Larsson, S.; Cassland, P.; Jonsson, L. J. Development of a *Saccharomyces cerevisiae* strain with enhanced resistance to phenolic fermentation inhibitors in lignocellulose hydrolysates by heterologous expression of laccase. *Appl. Environ. Microbiol.* **2001**, *67* (3), 1163–1170.
(9) Martin, C.; Marcet, M.; Almazan, O.; Jonsson, L. J. Adaptation of a recombinant xylose-utilizing *Saccharomyces cerevisiae* strain to a sugarcane bagasse hydrolysate with high content of fermentation inhibitors. *Bioresour. Technol.* **2007**, *98* (9), 1767–1773.
(10) Keating, J. D.; Panganiban, C.; Mansfield, S. D. Tolerance and adaptation of ethanologenic yeasts to lignocellulosic inhibitory compounds. *Biotechnol. Bioeng.* **2006**, *93* (6), 1196–1206.

(11) Martin, C.; Jonsson, L. J. Comparison of the resistance of industrial and laboratory strains of *Saccharomyces* and *Zygosaccharomyces* to lignocellulose-derived fermentation inhibitors. *Enzyme Microb. Technol.* **2003**, *32* (3−4), 386–395.
(12) Russell, N. J.; Evans, R. I.; terSteeg, P. F.; Hellemons, J.; Verheul, A.; Abee, T. Membranes as a target for stress adaptation. *Int. J. Food Microbiol.* **1995**, *28* (2), 255–261.
(13) Lei, J.; Zhao, X.; Ge, X.; Bai, F. Ethanol tolerance and the variation of plasma membrane composition of yeast floc populations with different size distribution. *J. Biotechnol.* **2007**, *131*, 270–275.
(14) Mannazzu, I.; Angelozzi, D.; Budroni, M.; Farris, G. A.; Gofffini, P.; Lodi, T.; Marzona, M.; Bardi, L.; Belviso, S. Behaviour of *Saccharomyces cerevisiae* wine strains during adaptation to unfavourable conditions of fermentation on synthetic medium: cell lipid composition, membrane integrity, viability and fermentative activity. *Int. J. Food Microbiol.* **2008**, *121*, 84–91.
(15) Wolf, C.; Quinn, P. J. Lipidomics: practical aspects and applications. *Prog. Lipid Res.* **2008**, *47*, 15–36.
(16) Gaspar, M. L.; Aregullin, M. A.; Jesch, S. A.; Nunez, L. R.; Villa-Garcia, M.; Henry, S. A. The emergence of yeast lipidomics. *Biochim. Biophys. Acta* **2007**, *1771* (3), 241–254.
(17) Klinke, H. B.; Thomsen, A. B.; Ahring, B. K. Potential inhibitors from wet oxidation of wheat straw and their effect on growth and ethanol production by *Thermoanaerobacter mathranii*. *Appl. Microbiol. Biotechnol.* **2001**, *57* (5−6), 631–638.
(18) Martinez, A.; Rodriguez, M. E.; Wells, M. L.; York, S. W.; Preston, J. F.; Ingram, L. O. Detoxification of dilute acid hydrolysates of lignocellulose with lime. *Biotechnol. Prog.* **2001**, *17* (2), 287–293.
(19) Folch, J.; Lees, M.; Sloane Stanley, G. H. A simple method for the isolation and purification of total lipides from animal tissues. *J. Biol. Chem.* **1957**, *226* (1), 497–509.
(20) Bligh, E. G.; Dyer, W. J. A rapid method of total lipid extraction and purification. *Can. J. Biochem. Physiol.* **1959**, *37* (8), 911–7.
(21) Guan, X. L.; Wenk, M. R. Mass spectrometry-based profiling of phospholipids and sphingolipids in extracts from *Saccharomyces cerevisiae*. *Yeast* **2006**, *23* (6), 465–477.
(22) Weerheim, A. M.; Kolb, A. M.; Sturk, A.; Nieuwland, R. Phospholipid composition of cell-derived microparticles determined by one-dimensional high-performance thin-layer chromatography. *Anal. Biochem.* **2002**, *302* (2), 191–198.
(23) Yang, S.; Qiao, B.; Lu, S. H.; Yuan, Y. J. Comparative lipidomics analysis of cellular development and apoptosis in two *Taxus* cell lines. *Biochim. Biophys. Acta* **2007**, *1771* (5), 600–612.
(24) Xia, J. M.; Wu, X. J.; Yuan, Y. J. Integration of wavelet transform with PCA and ANN for metabolomics data-mining. *Metabolomics* **2007**, *3*, 531–537.
(25) Wagner, S.; Paltauf, F. Generation of glycerophospholipid molecular-species in the yeast *Saccharomyces-cerevisiae*—fatty-acid pattern of phospholipid classes and selective acyl turnover at sn-1 and sn-2 positions. *Yeast* **1994**, *10* (11), 1429–1437.
(26) Daum, G.; Tuller, G.; Nemec, T.; Hrastnik, C.; Balliano, G.; Cattel, L.; Milla, P.; Rocco, F.; Conzelmann, A.; Vionnet, C.; Kelly, D. E.; Kelly, S.; Schweizer, E.; Schuller, H. J.; Hojad, U.; Greiner, E.; Finger, K. Systematic analysis of yeast strains with possible defects in lipid metabolism. *Yeast* **1999**, *15* (7), 601–614.
(27) Boumann, H. A.; Damen, M. J. A.; Versluis, C.; Heck, A. J. R.; de Kruijff, B.; de Kroon, A. The two biosynthetic routes leading to phosphatidylcholine in yeast produce different sets of molecular species. Evidence for lipid remodeling. *Biochemistry* **2003**, *42* (10), 3054–3059.
(28) Bankaitis, V. A.; Morris, A. J. Lipids and the exocytotic machinery of eukaryotic cells. *Curr. Opin. Cel.l Biol.* **2003**, *15* (4), 389–395.
(29) Ramos, J. L.; Duque, E.; Rodriguez-Herva, J. J.; Godoy, P.; Haidour, A.; Reyes, F.; Fernandez-Barrero, A. Mechanisms for solvent tolerance in bacteria. *J. Biol. Chem.* **1997**, *272* (7), 3887–3890.
(30) Payrastre, B.; Missy, K.; Giuriato, S.; Bodin, S.; Plantavid, M.; Gratacap, M. P. Phosphoinositides—key players in cell signalling, in time and space. *Cell. Signal.* **2001**, *13* (6), 377–387.
(31) Jesch, S. A.; Zhao, X.; Wells, M. T.; Henry, S. A. Genome-wide analysis reveals inositol, not choline, as the major effector of Ino2p-Ino4p and unfolded protein response target gene expression in yeast. *J. Biol. Chem.* **2005**, *280* (10), 9106–9118.
(32) Boumann, H. A.; Gubbens, J.; Koorengevel, M. C.; Oh, C. S.; Martin, C. E.; Heck, A. J. R.; Patton-Vogt, J.; Henry, S. A.; de Kruijff, B.; de Kroon, A. Depletion of phosphatidylcholine in yeast induces shortening and increased saturation of the lipid acyl chains: Evidence for regulation of intrinsic membrane curvature in a eukaryote. *Mol. Biol. Cell* **2006**, *17* (2), 1006–1017.
(33) Santiago, T. C.; Mamoun, C. B. Genome expression analysis in yeast reveals novel transcriptional regulation by inositol and choline and new regulatory functions for Opi1p, Ino2p, and Ino4p. *J. Biol. Chem.* **2003**, *278* (40), 38723–38730.
(34) Dixon, R. A.; Gang, D. R.; Charlton, A. J.; Fiehn, O.; Kuiper, H. A.; Reynolds, T. L.; Tjeerdema, R. S.; Jeffery, E. H.; German, J. B.; Ridley, W. P.; Seiber, J. N. Perspective—applications of metabolomics in agriculture. *J. Agric. Food Chem.* **2006**, *54*, 8984–8994.
(35) Turk, M.; Mejanelle, L.; Sentjurc, M.; Grimalt, J. O.; Gunde-Cimerman, N.; Plemenitas, A. Salt-induced changes in lipid composition and membrane fluidity of halophilic yeast-like melanized fungi. *Extremophiles* **2004**, *8* (1), 53–61.
(36) Bremer, J.; Greenberg, D. M. Biosynthesis of choline in vitro. *Biochim. Biophys. Acta* **1960**, *37* (1), 173–175.
(37) Kennedy, E. P.; Weiss, S. B. Function of cytidine coenzymes in the biosynthesis of phospholipids. *J. Biol. Chem.* **1956**, *222* (1), 193–213.
(38) Pepi, M.; Heipieper, H. J.; Fischer, J.; Ruta, M.; Volterrani, M.; Focardi, S. E. Membrane fatty acids adaptive profile in the simultaneous presence of arsenic and toluene in *Bacillus* sp ORAs2 and *Pseudomonas* sp ORAs5 strains. *Extremophiles* **2008**, *12* (3), 343–349.
(39) Ingram, L. O. Adaptation of membrane lipids to alcohols. *J. Bacteriol.* **1976**, *125* (2), 670–678.
(40) Del Castillo Agudo, L.; Nieto Soria, A.; Sentandreu, R. Differential expression of the invertase-encoding SUC genes in *Saccharomyces cerevisiae*. *Gene (Amsterdam)* **1992**, *120* (1), 59–65.
(41) Deyoung, L. R.; Dill, K. A. Solute partitioning into lipid bilayer-membranes. *Biochemistry* **1988**, *27*, 5281–5289.
(42) Rutters, H.; Sass, H.; Cypionka, H.; Rullkotter, J. Phospholipid analysis as a tool to study complex microbial communities in marine sediments. *J. Microbiol. Methods* **2002**, *48* (2−3), 149–160.
(43) Yang, S.; Lu, S. H.; Yuan, Y. J. Lipidomic analysis reveals differential defense responses of Taxus cuspidata cells to two elicitors, methyl jasmonate and cerium (Ce^{4+}). *Biochim. Biophys. Acta Mol. Cell. Biol. Lipids* **2008**, *1781* (3), 123–134.

Received for review September 3, 2008. Revised manuscript received November 8, 2008. Accepted November 10, 2008. We are very grateful for financial support from the National Science Fund of China for Distinguished Young Scholars Grant (Project 20425620), Key Program Grant (Project 20736006), the National Basic Research Program "973" of China (2007CB714301), and Key Projects in the National Science and Technology Pillar Program (2007BAD42B02).

JF802720T